ISSN 1063-7737, Astronomy Letters, 2014, Vol. 40, No. 6, pp. 372–381. © Pleiades Publishing, Inc., 2014.
Original Russian Text © N.S. Petrukhin, 2014, published in Pis'ma v Astronomicheskiĭ Zhurnal, 2014, Vol. 40, No. 6, pp. 416–425.

Kink Oscillations of Asymmetric Coronal Loops

N. S. Petrukhin*

National Research University, Higher School of Economics,
ul. Bol'shaya Pecherskaya 25/14, Nizhni Novgorod, 603155 Russia

Received June 24, 2013

Abstract—The free oscillations of coronal loops with a constant density and a variable magnetic field changing according to parabolic laws are investigated. Using our developed method, we derive the wave equations with constant coefficients that describe the kink oscillations of symmetric and asymmetric magnetic flux tubes. For such models, we obtain analytical expressions for the oscillation spectra and amplitudes as well as the magnitudes and directions of the displacements of the extrema of the fundamental and first modes relative to their values for homogeneous tubes. For the first mode of an asymmetric loop, we have determined the dependence of the coordinate displacement for the internal node on the ratios of the magnetic field strengths in its asymmetric parts and the ratio of the amplitudes at the extremum points.

DOI: 10.1134/S1063773714060073

Keywords: *reflectionless waves, magnetoacoustic waves, corona, coronal loops, kink oscillations.*

INTRODUCTION

The transverse displacements in coronal magnetic loops detected by TRACE were the first wave phenomenon clearly observed in the corona (Aschwanden et al. 1999; Nakariakov et al. 1999). These oscillations were interpreted as the fundamental mode of standing kink waves in magnetic flux tubes. Subsequently, the first and, not quite reliably, higher-order modes were detected (Verwichte et al. 2004; Van Doorsselaere et al. 2007; O'Shea et al. 2007). Transverse perturbations propagating along the magnetic field were also observed in fibrils (Okamoto et al. 2007) and chromospheric spicules (De Pontieu et al. 2007).

The detection of loop oscillations made the subject matter of coronal helioseismology one of the most topical in solar astrophysics. Many theoretical works appeared in which symmetric loop model were proposed and calculations, mostly numerical or approximate analytical ones, were performed for these models to study the properties of such oscillations (for a review, see Andries et al. 2009; Ruderman and Erdelyi 2009; Stepanov et al. 2012; De Moortel and Nakariakov 2012). Note the paper by Dymova and Ruderman (2006), in which analytical solutions were obtained for a model with a constant magnetic field and a density specified in a parabolic form. Verth (2007) and Verth and Erdelyi (2008) numerically and analytically studied the oscillations of a coronal loop with a constant density in which the magnetic field was specified by a quadratic function.

In this paper, we consider coronal loop models with a constant density and a variable magnetic field that, just as in Verth and Erdelyi (2008), changes according to parabolic laws. For a symmetric model, we derived a refined expression for the spectrum of kink oscillations and found simple analytical expressions for the displacements of the extrema of the first-mode amplitude.

In addition, we consider coronal loop models in which the magnetic field is asymmetric relative to the loop tops. The results of our recent studies, in which we showed that traveling waves that do not reflect off inhomogeneities could exist in a highly inhomogeneous medium, formed the basis for our work. The mathematical method of obtaining such solutions is related to the transformations of arguments and functions whereby, for example, the wave equation with variable coefficients under certain restrictions is reduced to hyperbolic equations with constant coefficients, so that the existence of reflectionless traveling waves becomes obvious. In particular, we did this for internal and surface waves in an incompressible fluid (Talipova et al. 2009), for vertically propagating acoustic waves in inhomogeneous compressible atmospheres of the Earth and the Sun (Petrukhin et al. 2011, 2012a–2012c), and for fast magnetoacoustic waves in coronal loops (Ruderman et al. 2013).

*E-mail: npetruhin@hse.ru

REFLECTIONLESS KING WAVES IN MAGNETIC FLUX TUBES

Let us investigate the fast magnetoacoustic kink waves propagating along a thin magnetic flux tube. Generally, the unperturbed parameters are assumed to vary only along the tube. Studies have shown (Van Doorsselaere et al. 2009) that the curvature with a curvature radius typical of coronal loops affects weakly the dispersion relations for kink waves. Therefore, we will assume the tube to be straight and located along the oz axis. Thus, the plasma density can be defined by the relation

$$\rho = \begin{cases} \rho_i; & r < R(z), \\ \rho_e; & r > R(z). \end{cases} \quad (1)$$

Here, $R(z)$ is the transverse tube radius, ρ_i and ρ_e are the plasma densities inside and outside the tube, respectively, which are constant quantities in this paper. The following equilibrium condition should be met at the boundary of the tube with the surrounding medium:

$$\frac{B_i^2}{8\pi} + P_i = \frac{B_e^2}{8\pi} + P_e, \quad (2)$$

where $B_{i,e}$ and $P_{i,e}$ are the magnetic field strength and the gas pressure inside and outside the tube, respectively. Since the inequality $\frac{P}{B^2/8\pi} \ll 1$ holds in the coronal plasma (Aschwanden 2005), it follows from Eq. (2) that

$$B_e \approx B_i \approx B. \quad (3)$$

Spruit (1981), Dymova and Ruderman (2006), and Ruderman et al. (2008) showed the propagation of kink waves in such a tube to be described by the wave equation

$$\frac{\partial^2 u}{\partial t^2} - c^2(z)\frac{\partial^2 u}{\partial z^2} = 0, \quad (4)$$

where $u = \frac{\eta}{R}$, η is the transverse displacement of the tube, and

$$c(z) = \frac{B}{\sqrt{2\pi(\rho_i+\rho_e)}} \quad (5)$$

is the kink wave speed.

Equation (4) contains the variable coefficient $c^2(z)$ and, hence, its solution generally describes the transformation of an incident wave into waves transmitted and reflected off the medium's inhomogeneities and does not break up into two independent solutions corresponding to traveling waves in opposite directions. The existence of noninteracting counterpropagating waves is trivial in the case of an equation with constant coefficients. Therefore, it is important to find the transformations that reduce Eq. (4) to an equation with constant coefficients. The basic idea of this method was discussed in our previous papers (Petrukhin et al. 2011, 2012a–2012c; Ruderman et al. 2013). We showed that these transformations brought the wave equation (4) to the form

$$\frac{\partial^2 \Phi}{\partial t^2} - \frac{\partial^2 \Phi}{\partial \tau^2} = \beta\Phi, \quad (6)$$

where

$$\Phi(t,\tau) = u(t,z)/\sqrt{c(z)}, \tau(z) = \int \frac{dz}{c(z)} \quad (7)$$

and β is an arbitrary constant. Equation (6) in variables $\Phi(t,\tau)$ describes the oppositely traveling noninteracting waves with the dispersion relation

$$\omega^2 = k^2 - \beta, \quad (8)$$

where ω is the wave frequency and k is the wave number relative to the new coordinate τ. In this case, the function $c(z)$ should satisfy, in particular, the condition

$$c = M(z+N)^2 + \beta/M, \quad (9)$$

where M and N are arbitrary constants. The models of coronal flux tubes described by Eq. (9) can be divided into two types. The first case, in which $M > 0$ and, consequently, $\beta > 0$, corresponds to a parabola with upward-directed branches. In this case, the speed $c(z)$ decreases with height. The second case ($M < 0$ and, consequently, $\beta < 0$) describes a family of parabolas with downward-directed branches. At such parameters, the kink wave speed $c(z)$ increases with height. In this paper, we consider the first case.

FREE OSCILLATIONS OF A SYMMETRIC LOOP WITH A CONSTANT DENSITY

Using Eq. (9), let us construct the models of solar coronal loops that consist of parabolic reflectionless profiles for the speed of kink waves. We consider only the part of the tube that is located above the photosphere. The magnetic field lines are closed in dense subphotospheric layers. Since the density is known to change abruptly at the photospheric height, we will assume this level to be a rigid reflecting boundary for the kink waves propagating in a coronal loop. Let us choose the oz axis along a tube of length $2L$ with the coordinate origin in the middle of it. Let us first consider the symmetric model with positive M and β. In this case, $N = 0$. Denoting $c(z=0) = c_0$, $c(z = \pm L) = c_t$, and $\alpha = c_t/c_0$, we obtain

$$c = c_o\left[1 + (\alpha - 1)\left(\frac{z}{L}\right)^2\right], \quad (10)$$

$$\beta = c_o^2\frac{(\alpha-1)}{L^2}. \quad (11)$$

Assuming that

$$\Phi = \psi(\tau)e^{i\omega t}, \tag{12}$$

we obtain an ordinary differential equation with constant coefficients:

$$\frac{d^2\psi}{d\tau^2} + (\omega^2 + \beta)\psi = 0. \tag{13}$$

The function $r(z)$ defining the transverse displacements of the tube is related to the solution of Eq. (13) by the relation

$$r = [c(z)]^{1/2}R(z)\psi(z) = \rho^{-\frac{1}{4}}\psi(z). \tag{14}$$

Given that the density here is assumed to be constant, the variables ψ and r coincide to within a constant factor. Therefore, the general solution of Eq. (13) can be written as

$$r[\tau(z)] = A\sin(k\tau) + D\cos(k\tau), \tag{15}$$

where A and D are arbitrary constants and k is the wave number satisfying the dispersion relation (8). The new variable τ is related to the physical coordinate z by Eq. (7) and for the kink speed profile (10) under consideration is defined explicitly:

$$\tau(z) = \int_0^z \frac{dz'}{c(z')} = \frac{L}{c_0\sqrt{(\alpha-1)}} \times \arctan\left(\frac{z}{L}\sqrt{\alpha-1}\right). \tag{16}$$

Since the problem is symmetric relative to the coordinate origin, the boundary conditions can be specified at one of the tube ends, for example, at $z = L$ and in the middle of it (i.e., at $z = 0$). For the fundamental mode and for all modes with an even number of nodes, we assume that

$$r[\tau = \tau(L)] = 0, \quad \frac{dr}{dz}[\tau = \tau(0)] = 0 \tag{17}$$

and for odd modes

$$r[\tau = \tau(L)] = 0, \quad r[\tau = \tau(0)] = 0. \tag{18}$$

Satisfying the boundary conditions (17) and (18), we obtain the spectrum of free kink oscillations of the tube

$$\Omega_n = \sqrt{(\alpha-1)}\sqrt{\frac{n^2}{(\arctan\sqrt{\alpha-1})^2} - \frac{4}{\pi^2}}, \quad n = 1, 2, \ldots \tag{19}$$

Here, $\Omega_n = \omega_n/\omega_0$, ω_n is the eigenfrequency of the nth-mode oscillations and $\omega_0 = \pi c_0/2L$ is the frequency of the fundamental mode in a homogeneous tube of length $2L$ whose kink speed is c_0. The value of the parameter α equal to one corresponds to a medium with a constant speed c. In this case, either the plasma density and the magnetic field are constant or they vary, compensating each other. The eigenfunctions for the eigenfrequencies can be written as

$$r_n = \begin{Bmatrix} A_n\cos \\ D_n\sin \end{Bmatrix}\left[\frac{\pi n \arctan(\frac{z\sqrt{\alpha-1}}{L})}{2\arctan\sqrt{\alpha-1}}\right] \times \begin{Bmatrix} n = 1, 3, \ldots \\ n = 2, 4, \ldots \end{Bmatrix}, \tag{20}$$

where A_n and D_n are arbitrary constants. The upper and lower expressions in curly brackets correspond to the even and odd modes, respectively.

The sign and magnitude of the deviation of the extrema of the oscillation amplitudes in a medium with variable parameters from their values in a homogeneous plasma are important characteristics in using the results of theoretical studies in helioseismology.

Verth (2007) and Verth and Erdelyi (2008) investigated the shape of the amplitudes for the fundamental and first modes of tube oscillations for the model under consideration. They showed that the oscillation amplitudes for the fundamental mode are located inside the cosine graph defining the oscillation amplitude in a homogeneous medium, while the extrema of the amplitudes for the first mode are displaced relative to the extrema of the sine function to the coordinate origin.

Equations (20) allow simple formulas for determining the displacements of the extrema for the first oscillation mode to be derived. Setting the argument of the sine function in the segments $[-L, 0]$ and $[0, L]$ equal to $\pm\frac{\pi}{2}$, respectively, we obtain

$$\left(\frac{z}{L}\right)_{\text{extr}} = \pm\frac{1}{1+\sqrt{\alpha}}, \tag{21}$$

where the plus and minus refer to the right and left halves of the loop, respectively. The deviation of the extrema from the middles of the segments is

$$\left(\frac{\triangle z}{L}\right)_{\text{extr}} = \pm\frac{1-\sqrt{\alpha}}{2(1+\sqrt{\alpha})}. \tag{22}$$

Since $\alpha > 1$ in the model under consideration, the influence of a magnetic field inhomogeneity causes the extrema of the amplitudes for the first mode to be displaced to the coordinate origin, i.e., in the direction of decreasing kink speed (10), as follows from the numerical studies by Verth (2007) and Verth and Erdelyi (2008).

FREE OSCILLATIONS OF AN ASYMMETRIC LOOP WITH A CONSTANT DENSITY

Consider the model of a coronal loop filled with a homogeneous plasma and consisting of two asymmetric parts that are connected at the top ($z = 0$) and rest on active regions with magnetic fields whose strengths differ. Let us specify a magnetic field in the form

$$B(z) = \begin{cases} B_1(z) \\ B_2(z) \end{cases} \tag{23}$$
$$= B(0) \begin{cases} 1 + (\alpha_1 - 1)\left(\frac{z}{L}\right)^2, & -L \le z \le 0 \\ 1 + (\alpha_2 - 1)\left(\frac{z}{L}\right)^2, & 0 \le z \le L, \end{cases}$$

where

$$\alpha_1 = B_1(-L)/B(0), \quad \alpha_2 = B_2(L)/B(0), \tag{24}$$
$$\beta_{1,2} = \frac{[B(0)]^2}{2\pi(\rho_i + \rho_e)} \frac{(\alpha_{1,2} - 1)}{L^2}.$$

In this case, the kink wave speed is proportional to the magnetic field strength:

$$c_{1,2}(z) \propto B_{1,2}(z). \tag{25}$$

Taking this into account, conditions (24) can be rewritten as

$$\alpha_1 = c_1(-L)/c_0, \quad \alpha_2 = c_2(L)/c_0, \tag{26}$$
$$\beta_{1,2} = c_0^2 \frac{(\alpha_{1,2} - 1)}{L^2}.$$

Making transformations in Eq. (4) for this model similar to those made in the previous section for a symmetric tube, we obtain

$$\frac{d^2\psi_{1,2}}{d\tau_{1,2}^2} + (\omega^2 + \beta_{1,2})\psi_{1,2} = 0, \tag{27}$$

where the indices 1 and 2 correspond to the segments $[-L, 0]$ and $[0, L]$, respectively. The new variables $\tau_{1,2}$ are related to the physical coordinate z by Eq. (7) and are defined explicitly as

$$\tau_{1,2} = \int_0^z \frac{dz'}{c_{1,2}} \tag{28}$$
$$= \frac{L}{c_0\sqrt{(\alpha_{1,2} - 1)}} \arctan\left(\frac{z}{L}\sqrt{\alpha_{1,2} - 1}\right).$$

Since the plasma density is constant, the functions $\psi_{1,2}$ are proportional to the transverse displacements of the tube $r_{1,2}$. Therefore, the general solution of Eq. (27) can be written as

$$r_{1,2}[\tau_{1,2}(z)] \tag{29}$$
$$= A_{1,2}\sin(k_{1,2}\tau_{1,2}) + D_{1,2}\cos(k_{1,2}\tau_{1,2}),$$

Here, $A_{1,2}$ and $D_{1,2}$ are arbitrary constants and $k_{1,2}$ are the wave numbers that, given the dispersion relation (8) and $\beta_{1,2}$ (26), are

$$k_{1,2} = \frac{c_0\sqrt{(1 - \alpha_{1,2})}}{L} Q^{(1,2)}, \tag{30}$$

$$Q^{(1,2)} = \sqrt{\frac{\Omega^2\pi^2}{4(\alpha_{1,2} - 1)} + 1}, \quad \Omega = \frac{\omega}{\omega_0}. \tag{31}$$

We will assume the tube ends to be stationary. In addition, we will require that functions (29) and their first derivatives be continuous at the conjugation points ($z = 0$). Satisfying these boundary conditions, we find the dispersion relation for standing waves

$$\tan(Q_n^{(1)}\sqrt{\alpha_1 - 1})\cot(Q_n^{(2)}\arctan\sqrt{\alpha_2 - 1}) \tag{32}$$
$$= -\frac{Q_n^{(1)}\sqrt{\alpha_1 - 1}}{Q_n^{(2)}\sqrt{\alpha_2 - 1}}.$$

Here,

$$Q_n^{(1,2)} = \sqrt{\frac{\Omega_n^2\pi^2}{4(\alpha_{1,2} - 1)} + 1}, \quad \Omega_n = \frac{\omega_n}{\omega_0}. \tag{33}$$

The amplitudes corresponding to the oscillation eigenfrequencies are defined by the formulas

$$r_n = C_n \tag{34}$$
$$\times \begin{cases} \frac{\sin\left[Q_n^{(1)}\left(\arctan\sqrt{\alpha_1 - 1} + \arctan\left(\frac{z}{L}\sqrt{\alpha_1 - 1}\right)\right)\right]}{\sin\left[Q_n^{(1)}\left(\arctan\sqrt{\alpha_1 - 1}\right)\right]}, \\ -L \le z \le 0, \\ \frac{\sin\left[Q_n^{(2)}\left(\arctan\sqrt{\alpha_2 - 1} - \arctan\left(\frac{z}{L}\sqrt{\alpha_2 - 1}\right)\right)\right]}{\sin\left[Q_n^{(2)}\left(\arctan\sqrt{\alpha_2 - 1}\right)\right]}, \\ 0 \le z \le L, \end{cases}$$

where C_n are arbitrary constants.

The Model of a Loop with a Constant Magnetic Field in Half of It

Consider the model of an asymmetric loop in the left half of which the magnetic field does not vary, i.e., $\alpha_1 = 1$ and in the right half decreases from the footpoints to the top. Denote $\alpha_2 = \alpha > 1$. In this case, the dispersion relation (32) and eigenfunctions (34) can be rewritten as

$$\tan\left(\frac{\pi\Omega_n}{2}\right)\cot(Q_n\arctan\sqrt{\alpha - 1}) \tag{35}$$
$$= -\frac{\pi\Omega_n}{2}\frac{1}{Q_n\sqrt{\alpha - 1}},$$

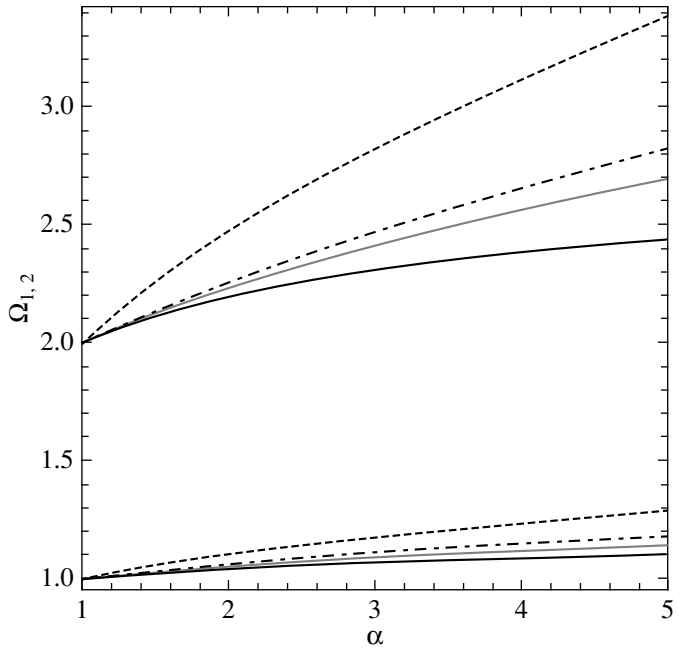

Fig. 1. Frequencies $\Omega_{1,2}$ of the fundamental and first modes versus parameter α.

$$Q_n = \sqrt{\frac{\Omega_n^2\pi^2}{4(\alpha-1)} + 1},$$
$$n = 1, 2, ...$$

$$r_n = C_n \tag{36}$$
$$\times \begin{cases} \frac{\sin\frac{\pi\Omega_n}{2}(1+\frac{z}{L})}{\sin(\frac{\pi\Omega_n}{2})}, \\ -L \le z \le 0, \\ \frac{\sin\left[Q_n\left(\arctan\sqrt{\alpha-1} - \arctan\left(\frac{z}{L}\sqrt{\alpha-1}\right)\right)\right]}{\sin\left[Q_n\left(\arctan\sqrt{\alpha-1}\right)\right]}, \\ 0 \le z \le L. \end{cases}$$

For this model, the thick lines in Fig. 1 plot the relative frequencies of the fundamental and first modes against the parameter α. The plots of functions (19) for symmetric models are shown for comparison. The dashed lines are for the argument α and the dash–dotted lines are for the mean loop inhomogeneity parameters, i.e., $0.5(1+\alpha)$. Finally, the thin solid lines are constructed for the functions $[\Omega_{1,2}(\alpha) + \Omega_{1,2}(1)]/2$, which are the mean values for the frequencies of the homogeneous and corresponding inhomogeneous symmetric models. It can be seen from the figure that the oscillation frequencies for both fundamental and first modes of the asymmetric model are lower than those for the above symmetric models. In addition, at identical parameters α, they are also lower than $[\Omega_{1,2}(\alpha) + \Omega_{1,2}(1)]/2$.

Figure 2 plots the amplitudes of the fundamental mode (36) for an asymmetric loop for α from 1 to 4 with a step of 1. At $\alpha = 1$, the loop is symmetric

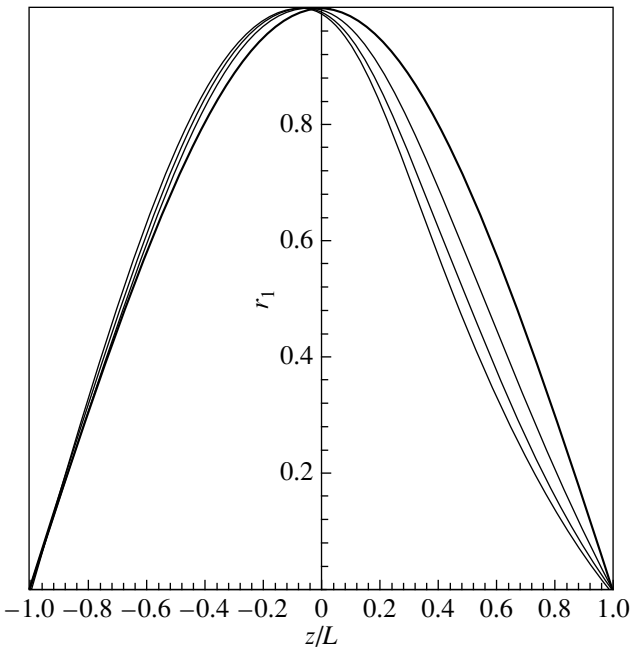

Fig. 2. Amplitudes of the fundamental mode (36) for α from 1 to 4 with a step of 1. The thick line is a cosine wave ($\alpha = 1$).

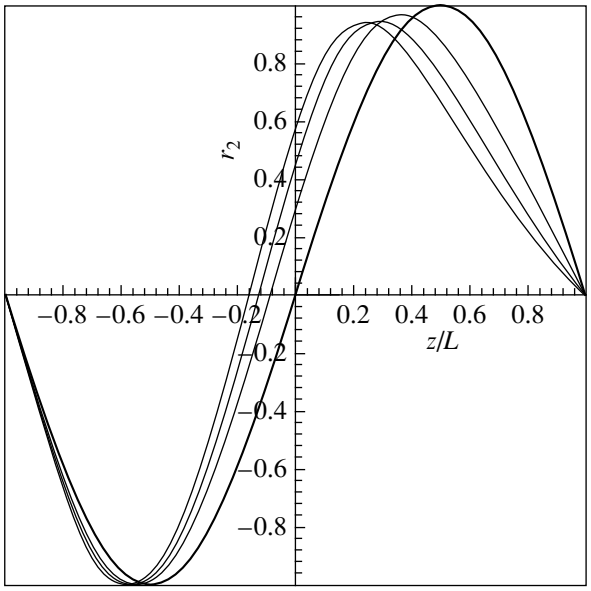

Fig. 3. Amplitudes of the first mode (36) for α from 1 to 4 with a step of 1. The thick line is a sine wave ($\alpha = 1$).

and homogeneous; the graph of the amplitude of its fundamental mode is a cosine wave. In Fig. 2, it is highlighted by the thick line. It can be seen from these plots that the maxima of the amplitudes of free oscillations for the asymmetric tube are displaced toward a weaker magnetic field, with the displacement increasing with parameter α. It is also interesting to note that, just as in the symmetric model, the curves are located "inside" and "outside" the cosine wave in the right inhomogeneous and left homogeneous parts of the plot, respectively.

An analytical expression for the coordinate at which the amplitude of the fundamental mode is at a maximum can be easily derived from Eq. (36) for $-L \le z \le 0$ by setting the argument of the sine function equal to $\pi/2$:

$$\left(\frac{z}{L}\right)^{(1)}_{\max} = \frac{1-\Omega_1}{\Omega_1}. \tag{37}$$

Figure 3 presents the amplitudes of the first mode (38) for the same parameters as those in Fig. 2. The sine graph is highlighted by the thick line. The extrema of the amplitudes for the first mode are known to be symmetric relative to the coordinate origin in the symmetric model. In the asymmetric case, the picture is qualitatively different.

First, the graph of the amplitude is asymmetric. The internal node is displaced from the coordinate origin leftward, i.e., toward a weaker magnetic field. In this case, the node coordinate can be easily determined from Eq. (36):

$$\left(\frac{z}{L}\right)_{\text{node}} = \frac{2-\Omega_2}{\Omega_2}. \tag{38}$$

Second, the displacements of the extrema are asymmetric relative to the node; in this case, in contrast to the symmetric case, they are displaced from the middles of the segments $-L \le z \le 0$ and $0 \le z \le L$ in the same direction. Analytical expressions for these displacements can also be easily found from Eqs. (36). The deviation of the amplitude minimum from the middle of the segment $-L \le z \le 0$ is

$$\left(\frac{\triangle z}{L}\right)_{\min} = \frac{2-\Omega_2}{2\Omega_2}. \tag{39}$$

Since the frequency of the first mode $\Omega_2 > 2$, the minimum of its amplitude is displaced toward the left footpoint of the tube. As follows from Fig. 3, the deviation of the maximum corresponding to the part of the loop with a variable magnetic field exceeds appreciably in magnitude the displacement of the minimum. The maximum point can be determined using the expression

$$\left(\frac{z}{L}\right)_{\max} = \frac{1-\frac{\tan\varphi_2}{\sqrt{\alpha-1}}}{1+\sqrt{\alpha-1}\tan\varphi_2} \cong \frac{\Omega_2-1}{\alpha-1+\Omega_2}, \tag{40}$$

where $\varphi_2 = \frac{\pi}{2Q_2}$. Here, in addition to the exact formula, its approximate value is presented (the relative error for the inhomogeneity parameters α under consideration is less than 8%), which allows a simple dependence of the deviation of the amplitude maximum from the middle of the segment $0 \le z \le L$ on frequency and parameter α to be written:

$$\left(\frac{\triangle z}{L}\right)_{\max} \cong \frac{\Omega_2-(\alpha+1)}{2(\Omega_2+\alpha-1)}. \tag{41}$$

Using the dispersion relation (19), it can be shown that $\Omega_2(\alpha) < \alpha+1$; therefore, the displacement of the right maximum, just as the left one, is negative.

Third, the maximum values of the amplitudes in the left and right parts of the same curve are unequal. The left extremum exceeds the right one in absolute value and their ratio is

$$\left|\frac{r_2[(\frac{z}{L})_{\min}]}{r_2[(\frac{z}{L})_{\max}]}\right| = \left|\frac{\sin\left[Q_2\left(\arctan\sqrt{\alpha-1}\right)\right]}{\sin\left(\frac{\pi\Omega_2}{2}\right)}\right|, \tag{42}$$

and this difference increases with parameter α.

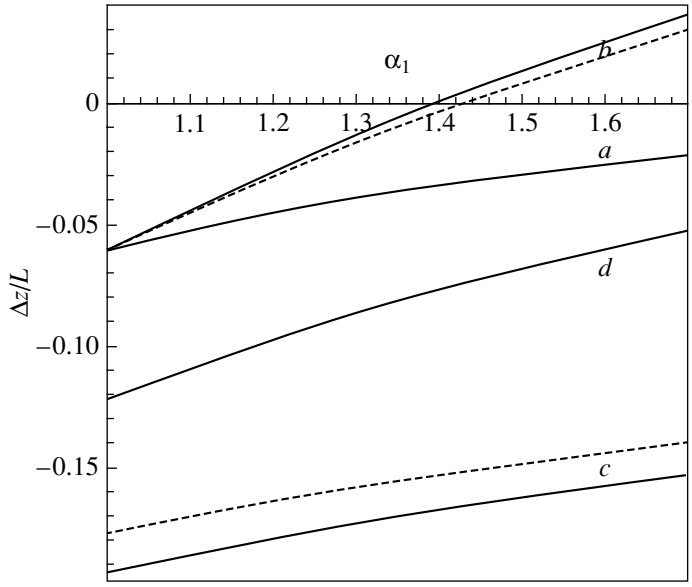

Fig. 4. Displacements $\triangle z/L$ of the nodes and extrema of the fundamental and first modes from their values in homogeneous tubes at constant $\alpha_2 = 2.676$ versus parameter α_1. Curve *a* is for the fundamental mode, curves *b* and *c* are for the minima and maxima of the first mode, respectively, and curve *d* is for the internal nodes of the first mode. The solid and dashed curves represent the exact and approximate values, respectively.

The Model of a Loop with a Variable Magnetic Field over Its Whole Length

Consider an asymmetric tube with a variable magnetic field in each of its halves. Let the inhomogeneity parameter be α_1 and α_2 in the left and right parts of the tube, respectively. To be specific, we will assume that $\alpha_2 > \alpha_1$. It has been shown above that higher relative frequencies Ω correspond to larger values of the parameter α. It follows from Eqs. (30) and (31) that this property will be also valid for the wave numbers

$$k(\alpha_2) > k_n(\alpha_1, \alpha_2) > k_n(\alpha_1), \qquad (43)$$

where $k_n(\alpha_{1,2})$ are the wave numbers corresponding to the oscillation eigenfrequencies (19) for symmetric tubes. This implies that the wave in the half of the tube with a smaller α_1 is shorter than that in its other half. Therefore, the maximum of the amplitude for the fundamental mode will be displaced from the coordinate origin toward negative values of the argument, i.e., toward smaller magnetic field strengths. The magnitude of this displacement can be obtained by setting the argument of the sine function in (34) in the segment $-L < z < 0$ equal to $\frac{\pi}{2}$. As a result, we find that

$$\left(\frac{z}{L}\right)^{(1)}_{\max} = \frac{\frac{\tan\varphi_1^{(1)}}{\sqrt{\alpha_1-1}} - 1}{1 + \sqrt{\alpha_1 - 1}\tan\varphi_1^{(1)}} \qquad (44)$$

$$\cong \frac{\varphi_1^{(1)} - \arctan\sqrt{\alpha_1 - 1}}{\sqrt{\alpha_1 - 1}},$$

where $\varphi_1^{(1)} = \frac{\pi}{2Q_1^{(1)}}$. Our estimates show that for the most interesting (for observations) cases where the parameters $\alpha_{1,2}$ vary within the range from 1 to 4 (i.e., the transverse radius of the coronal tube increases from 1 to 2), $(\frac{z}{L})^{(1)}_{\max} \ll 1$ and the exact and approximate values of (44) virtually coincide. This can be clearly seen from Fig. 4, where the plots of these functions are represented by curves *a*, which merge into a single line. The displacements of the maxima decrease in absolute value with decreasing difference of the parameters α_2 and α_1 and become zero at their equality. Let us determine the coordinates of the internal node and the extrema of the first mode. It follows from inequalities (43) that the node $(\frac{z}{L})^{(2)}_{\text{node}}$ will be displaced from the middle of the tube leftward. The magnitude of this displacement can be obtained by setting the argument of the sine function in (34) in the segment $-L < z < 0$ equal to π. Thus, the coordinate of the internal node of the first mode will also be defined by Eqs. (44), in which $\varphi_1^{(1)}$ should be replaced by $\varphi_2 = \frac{\pi}{Q_2^{(1)}}$. The merging plots of these functions are designated by curve *d* in Fig. 4.

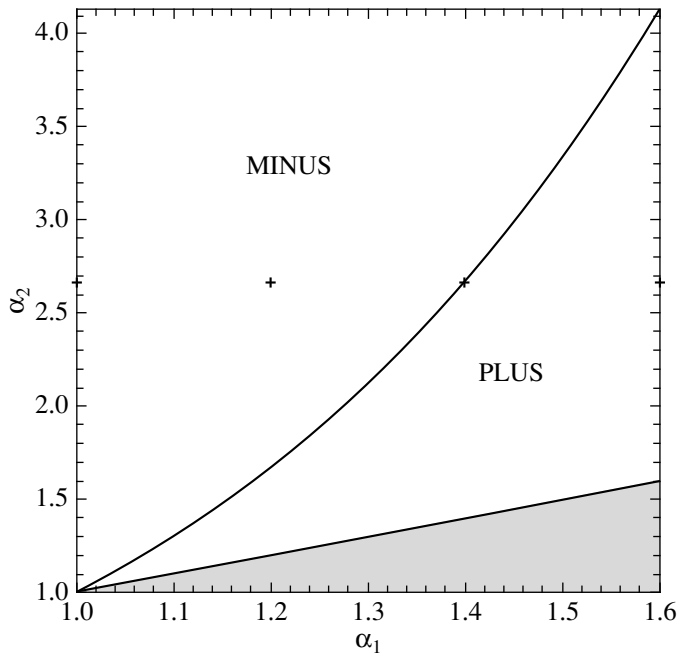

Fig. 5. Plot of the curve $F(\alpha_1, \alpha_2) = 0$, where α_1 and α_2 are the values at which the minimum of the oscillation amplitude for the first mode (34) is $-0.5z/L$. The MINUS and PLUS fields are the negative and positive displacements, respectively. The + sign marks the parameters for which the plots in Fig. 6 were constructed. The shaded region is $\alpha_1 > \alpha_2$.

The extrema of the amplitudes are defined by relations similar to Eqs. (40):

$$\left(\frac{z}{L}\right)^{(1,2)}_{(\max)} = \pm\frac{\frac{\tan\varphi_2^{(1,2)}}{\sqrt{\alpha_{1,2}-1}} - 1}{1 + \sqrt{\alpha_{1,2}-1}\tan\varphi_2^{(1,2)}} \cong \pm\frac{1-\Omega_2^{(1,2)}}{\alpha_{(1,2)} - 1 + \Omega_2^{(1,2)}}, \quad (45)$$

where the + sign and the index 1 refer to the left minimum, while the − sign and the index 2 refer to the right maximum and $\varphi_2^{(1,2)} = \frac{\pi}{2Q_2^{(1,2)}}$. The magnitude and direction of the displacement of the extrema for the amplitude of the first mode are affected by two factors. First, the extrema are displaced to the loop top, because the magnetic field is nonuniform. For a symmetric tube, this displacement is defined by Eqs. (21). Second, loop asymmetry leads to amplitude deformation, which is manifested as a deviation of both extrema toward a weaker magnetic field. Thus, both factors act in the same direction in the half of the tube with a stronger magnetic field, while their actions in the part of the tube where the magnetic field is weaker are opposite. In particular, in the half of the tube with a weaker magnetic field for certain relations between the parameters α_1 and α_2, these two types of displacements can completely cancel each other out. Figure 5 presents a diagram that shows the curve $F(\alpha_1, \alpha_2) = 0$. The coordinates of the points lying on this curve correspond to the values of α_1 and α_2 at which such cancelation occurs. A fairly accurate (with a relative error of $\sim$1%) expression for the eigenfrequency corresponding to such values of the parameters can be easily derived using the approximate formula (45). It has a simple form:

$$\Omega_2 \cong \alpha_1 + 1. \quad (46)$$

The fields of the diagram to the left and the right of the curve contain the parameters at which the amplitude minimum is displaced relative to the point $-0.5z/L$ in the negative and positive directions, respectively. In this case, the frequencies are lower than (46) in the left part and higher in the right one. The shaded region of the diagram corresponds to the values for which the inequality $\alpha_1 > \alpha_2$ holds.

Figure 6 shows the oscillation amplitudes of the first mode (34) for the loop model for α_1 changing from 1 to 1.6 with a step of 0.2. For all curves (except the thick line), $\alpha_2 = 2.676$. For the dash–dotted line, $\alpha_1 = 1$. The dashed line ($\alpha_1 = 1.4$) corresponds to the amplitude whose minimum lies at the point $-0.5z/L$. For comparison, the thick line represents a sine wave ($\alpha_1 = \alpha_2 = 1$). The + sigh in Fig. 5 marks the points corresponding to the parameters α_1 and α_2 for which the plots of the amplitudes were

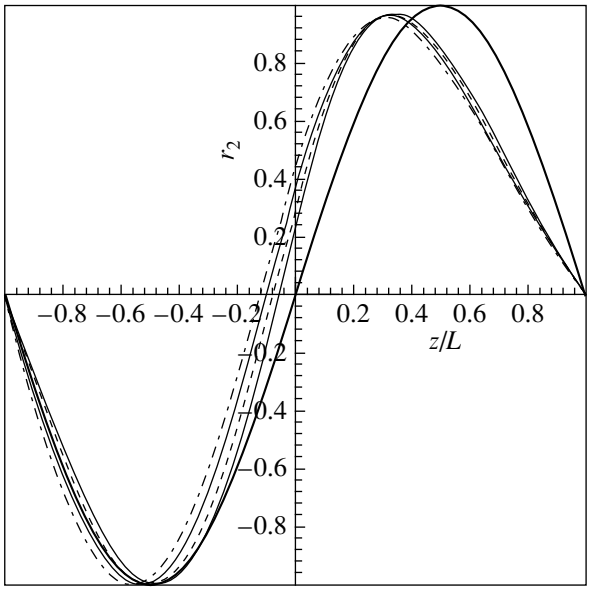

Fig. 6. Amplitudes of the first mode (44) for α_1 from 1 to 1.6 with a step of 0.2. For all curves (except the thick line), $\alpha_2 = 2.676$. For the dash–dotted line, $\alpha_1 = 1$. The dashed line corresponds to the amplitude whose minimum lies at the point $(-0.5z/L, 0)$. The thick line is a sine wave ($\alpha_1 = \alpha_2 = 1$).

constructed. First of all, note that the extrema of the amplitudes of the first mode for the asymmetric model have different values. In the part of the loop where the magnetic field is weaker, the amplitude is larger. The ratio of the amplitudes at the extrema is defined by the formula

$$\left|\frac{r_2[(\frac{z}{L})_{\min}]}{r_2[(\frac{z}{L})_{\max}]}\right| = \left|\frac{\sin\left[Q_2\left(\arctan\sqrt{\alpha_2-1}\right)\right]}{\sin\left[Q_1\left(\arctan\sqrt{\alpha_1-1}\right)\right]}\right|. \quad (47)$$

It also follows from Fig. 6 that the the displacement of the node and extrema is largest for the loop model in which the magnetic field does not change ($\alpha_1 = 1$) in one of its halves. If the magnetic field is variable over the whole length of an asymmetric tube, then the absolute value of the displacement of the internal node and the right maximum relative to their values in a homogeneous medium increases with increasing difference of the magnetic fields at its footpoints. A similar picture is also observed for the extremum in the part of the tube with a weaker magnetic field. In this case, however, the displacement is measured not from $-0.5z/L$ but from the negative value of (21) that is the coordinate of the minimum in a symmetric loop with an inhomogeneity parameter equal to α_1.

CONCLUSIONS

We carried out mostly analytical studies of the free kink oscillations in symmetric and asymmetric coronal loops with a variable magnetic field filled with a homogeneous plasma. The method of reflectionless wave propagation that we proposed, which allows the wave equations in inhomogeneous media to be reduced to equations with constant coefficients at certain restrictions, formed the basis for our studies.

For symmetric models, we obtained a refined spectrum of free oscillations and found simple formulas defining the magnitude and direction of the displacement of the extrema for the first mode relative to their values for a homogeneous model.

We investigated the oscillations of asymmetric loops resting on regions with magnetic fields differing in absolute value. Two models were considered. In the first model, it is assumed that the magnetic field is constant in one half of the loop and changes in the other half, decreasing from the footpoints to the top. In the second model, the magnetic field is variable over the whole tube length. For each case, we derived the dispersion relations and investigated the shape of the amplitudes for the fundamental and first modes. We derived exact and simple approximate formulas describing the displacements of characteristic points (extrema and nodes) for the oscillation amplitudes from their values for the homogeneous model. The oscillation amplitudes of the first mode in the asymmetric model were shown to differ in magnitude, with the amplitude in the part of the loop with a weaker magnetic field being larger.

ACKNOWLEDGMENTS

This work was supported by the Russian Foundation for Basic Research (project no. 13-02-00656) and the Science Foundation of the Higher School of Economics of the National Research University.

REFERENCES

1. J. Andries, T. van Doorsselaere, B. Roberts, et al., Space Sci. Rev. **149**, 3 (2009).
2. M. J. Aschwanden, *Physics of the Solar Corona. An Introduction with Problems and Solutions* (Springer, Berlin, 2005), p. 909.
3. M. J. Aschwanden, L. Fletcher, C. J. Schrijver, et al., Astrophys. J. **520**, 880 (1999).
4. T. van Doorsselaere, E. Verwichte, and J. Terradas, Space Sci. Rev. **149**, 299 (2009).
5. T. van Doorsselaere, V. Nakariakov, and E. Verwichte, Astron. Astrophys. **473**, 959 (2007).
6. M. V. Dymova and M. S. Ruderman, Astron. Astrophys. **457**, 1059 (2006).
7. I. de Moortel and V. M. Nakariakov, Phil. Trans. R. Soc. A **370**, 3193 (2012).
8. V. Nakariakov, L. Ofman, E. E. DeLuca, et al., Science **285**, 862 (1999).
9. T. J. Okamoto, S. Tsuneta, T. E. Berge, et al., Science **318**, 1577 (2007).

10. E. O'Shea, A. K. Srivastava, J. G. Doyle, et al., Astron. Astrophys. **473**, 13 (2007).
11. N. S. Petrukhin, E. N. Pelinovsky, and E. K. Batsyna, JETP Lett. **93**, 564 (2011).
12. N. S. Petrukhin, E. N. Pelinovsky, and T. G. Talipova, Izv., Atmos. Ocean. Phys. **48**, 169 (2012a).
13. N. S. Petrukhin, E. N. Pelinovsky, and E. K. Batsyna, Astron. Lett. **38**, 388 (2012b).
14. N. S. Petrukhin, E. N. Pelinovsky, and E. K. Batsyna, Geomagn. Aeron. **52**, 814 (2012c).
15. B. de Pontieu, S. W. McIntosh, M. Carlsson, et al., Science **318**, 1574 (2007).
16. M. Ruderman, S. G. Verth, and R. Erdelyi, Astrophys. J. **686**, 684 (2008).
17. M. S. Ruderman and R. Erdelyi, Space Sci. Rev. **149**, 199 (2009).
18. M. S. Ruderman, E. Pelinovsky, N. S. Petrukhin, et al., Solar Phys. **286**, 417 (2013).
19. H. C. Spruit, Astron. Astrophys. **98**, 155 (1981).
20. A. V. Stepanov, V. V. Zaitsev, and V. M. Nakaryakov, Phys. Usp. **55**, 929 (2012).
21. T. G. Talipova, E. N. Pelinovsky, and N. S. Petrukhin, Oceanology **49**, 622 (2009).
22. G. Verth, Astron. Nachr. **328**, 764 (2007).
23. G. Verth and R. Erdelyi, Astron. Astrophys. **486**, 1015 (2008).
24. E. Verwichte, V. M. Nakariakov, L. Ofman, et al., Solar Phys. **223**, 77 (2004).

Translated by V. Astakhov